27. T. Odorisio, T. A. Rodriguez, E. P. Evans, A. R. Clarke, P. S. Burgoyne, *Nat. Genet.* **18**, 257 (1998).
28. H. Hall, P. Hunt, T. Hassold, *Curr. Opin. Genet. Dev.* **16**, 323 (2006).
29. This work was supported by NIH grant R01 HD040916 (M.J. and S.K); International Grants in Cancer Research (AIRC) [My First AIRC Grant (MFAG) grant 4765], Italian Ministry for Education, University and Research (MIUR), the Lalor Foundation, and the American-Italian Cancer Foundation (AICF) (M.B.); and the Charles H. Revson Foundation (F.B.). We thank M. Leversha [Memorial Sloan-Kettering Cancer Center (MSKCC)], P. Bois (Scripps Florida), and K. Manova (MSKCC) for valuable advice and protocols. We are grateful to Keeney and Jasin lab members, especially I. Roig, E. de Boer, and F. Cole, and to N. Hunter (University of California, Davis) for insightful comments.

Supporting Online Material
www.sciencemag.org/cgi/content/full/331/6019/916/DC1
SOM Text
Materials and Methods
Figs. S1 to S7
References

28 July 2010; accepted 21 December 2010
10.1126/science.1195774

Classic Selective Sweeps Were Rare in Recent Human Evolution

Ryan D. Hernandez,[1]* Joanna L. Kelley,[1] Eyal Elyashiv,[2] S. Cord Melton,[1] Adam Auton,[3] Gilean McVean,[3,4] 1000 Genomes Project, Guy Sella,[2]† Molly Przeworski[1,5,6]†‡

Efforts to identify the genetic basis of human adaptations from polymorphism data have sought footprints of "classic selective sweeps" (in which a beneficial mutation arises and rapidly fixes in the population). Yet it remains unknown whether this form of natural selection was common in our evolution. We examined the evidence for classic sweeps in resequencing data from 179 human genomes. As expected under a recurrent-sweep model, we found that diversity levels decrease near exons and conserved noncoding regions. In contrast to expectation, however, the trough in diversity around human-specific amino acid substitutions is no more pronounced than around synonymous substitutions. Moreover, relative to the genome background, amino acid and putative regulatory sites are not significantly enriched in alleles that are highly differentiated between populations. These findings indicate that classic sweeps were not a dominant mode of human adaptation over the past ~250,000 years.

Humans have experienced myriad adaptations since the common ancestor with chimpanzees and more recently have adapted to a wide range of environments. Efforts to infer the molecular basis of these adaptations from polymorphism data have largely been guided by the "classic selective sweep" model, in which a new, strongly beneficial mutation increases in frequency to fixation in the population [reviewed in (*1*, *2*)]. In this scenario, the allele ascends rapidly enough in frequency for there to be little opportunity for recombination to uncouple it from its genetic background, such that its rise sweeps out variation at linked sites, reducing linked neutral diversity in the population and distorting allele frequencies and patterns of linkage disequilibrium (*3*). In humans, the effects of sweeps are expected to persist for approximately 10,000 generations or about 250,000 years (*4*).

Identifying the footprint of a sweep against a noisy genomic background is challenging, because patterns of genetic variation reflect the effects of multiple modes of natural selection as well as of demographic history, mutation, and recombination. To date, applications of statistical tests based on the sweep model have led to the identification of more than 2000 genes as potential targets of positive selection in the human genome (*2*) and to the suggestion that diversity patterns in ~10% of the human genome have been affected by linkage to recent sweeps [e.g., (*5*)]. The list of functionally characterized cases of genetic adaptations is short, however, and the false discovery rate of selection scans is potentially high (*6*). Thus, it remains unknown whether the well-documented cases are typical of human adaptations, or whether they represent rare instances where the genetic architecture of the adaptation was conducive to classic sweeps (*7*, *8*), with most adaptations occurring by other modes (e.g., polygenic selection and selection on standing variation).

Two main lines of evidence have been advanced in support of the hypothesis that classic selective sweeps were common. First, regions of low recombination, in which a single sweep should have a larger span, exhibit lower diversity (after correcting for variation in mutation rates) relative to regions of high recombination (*9*–*11*). Regions of low recombination also show greater differentiation between populations (*12*), as expected from local adaptation or, for some parameters, from the fixation of globally advantageous alleles (*13*). Second, under the sensible assumption that amino acid and conserved noncoding sites are enriched among targets of adaptation, one would expect that the signal of selection would be most clearly visible at or around such sites [e.g., (*10*, *14*)]. Consistent with this expectation, diversity levels decrease with the number of human-specific substitutions at amino acid or conserved noncoding sites (in 200- to 600-kb windows) (*10*), and genic regions show an enrichment of alleles that are highly differentiated between populations relative to nongenic regions (*15*, *16*). These patterns are informative but are only indirectly related to theoretical predictions. Moreover, some—possibly all—of these patterns may instead result from purifying selection acting on deleterious mutations at linked sites ("background selection") (*9*–*11*, *16*–*18*).

To evaluate the importance of classic sweeps in shaping human diversity, we analyzed resequencing data for 179 human genomes from four populations, collected as part of the low-coverage pilot for the 1000 Genomes Project (*19*). These data overcome ascertainment biases arising in the study of genotyping data, with ~99% power to detect variants with a population frequency above 10% for 86% of the euchromatic genome (*19*).

We examined the extent to which selection affects diversity levels at linked sites by calculating the average diversity as a function of genetic distance from the nearest exons, collating all exons across the genome (fig. S1). To estimate neutral diversity levels, we focused only on nonconserved noncoding and fourfold degenerate sites (*11*). To correct for systematic variation in the mutation rate, we divided diversity by human–rhesus macaque divergence [to which the contribution of ancestral polymorphism is minor (*11*)]. Our estimate of relative diversity appears little affected by the low fold coverage of individuals or variation in sequencing depth (fig. S2, C to E). Scaled diversity levels are lowest near exons (Fig. 1A and fig. S3), recovering half the drop by 0.03 to 0.04 cM, depending on the population, and 80% by 0.07 to 0.1 cM [see (*20*)]. Given that diversity is scaled by divergence, the trough in scaled diversity around exons does not reflect systematic variation in mutation rates as a function of the distance from exons, strong purifying selection on the sites themselves (which would decrease both diversity and divergence), or weak selection near exons (which should inflate, not decrease, diversity levels divided by divergence). Rather, the trough provides evidence for the effects of directional selection at linked sites, extending over 100 kb.

[1]Department of Human Genetics, University of Chicago, Chicago, IL 60637, USA. [2]Department of Ecology, Evolution and Behavior, Hebrew University of Jerusalem, Givat Ram, Jerusalem 91904, Israel. [3]Wellcome Trust Centre for Human Genetics, University of Oxford, Oxford OX3 7BN, UK. [4]Department of Statistics, University of Oxford, Oxford OX1 3TG, UK. [5]Department of Ecology and Evolution, University of Chicago, Chicago, IL 60637, USA. [6]Howard Hughes Medical Institute, University of Chicago, Chicago, IL 60637, USA.

*Present address: Department of Bioengineering and Therapeutic Sciences, University of California, San Francisco, CA 94143, USA.
†These authors contributed equally to this work.
‡To whom correspondence should be addressed. E-mail: mfp@uchicago.edu

This pattern is even more pronounced on the X chomosome, where the trough is deeper and wider, recovering diversity over twice the genetic distance (Fig. 1C and fig. S3). The greater footprint of linked selection on the X leads to a smaller ratio of X to autosome scaled diversity near exons than farther away, potentially confounding demographic analysis (*21*) (fig. S4).

A similar effect is seen around conserved noncoding regions (CNCs), but the trough is more diffuse (Fig. 1, B and D, and fig. S3). Because CNCs tend to be linked to exons (the median distance of a CNC to the nearest exon is 0.08 cM), the trough around CNCs could be a by-product of the effects of selection on exons (see below); alternatively, it could reflect less widespread selection on mutations in CNCs relative to exons (*11*, *22*).

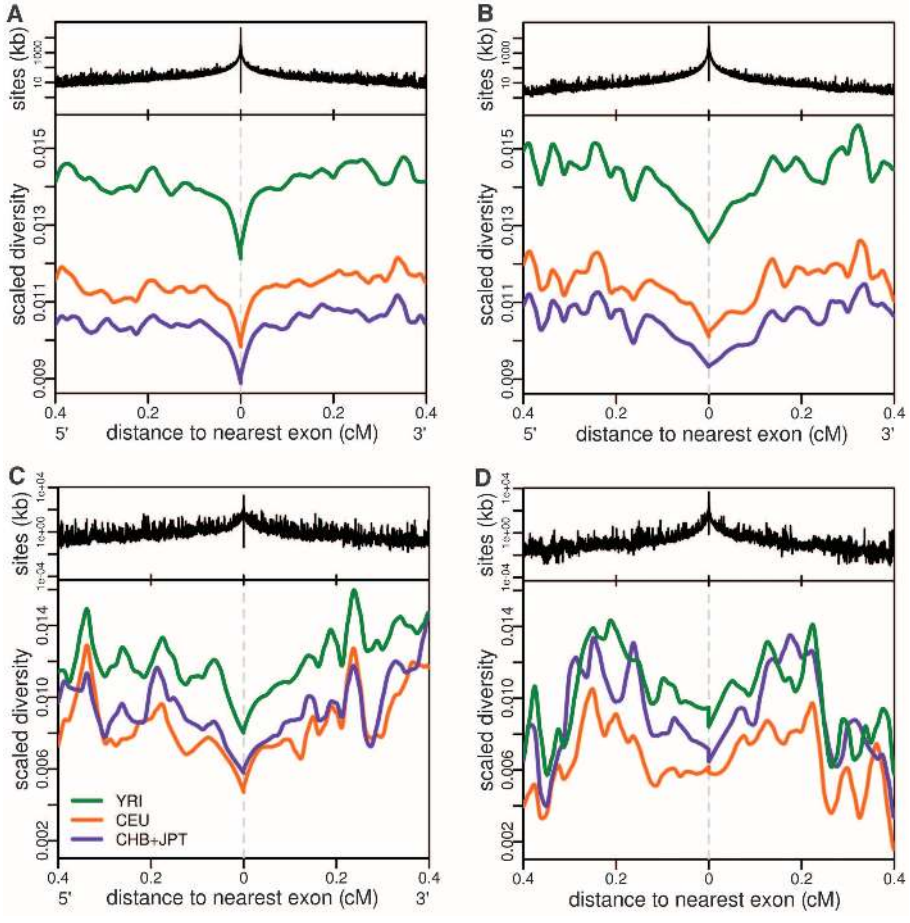

Fig. 1. (**A** to **D**) Diversity levels divided by human–rhesus macaque divergence (at nonconserved, noncoding sites) as a function of genetic distance from exons [(A) and (C)] and from conserved noncoding regions [(B) and (D)]. Autosome data are shown in (A) and (B); X chromosome data are shown in (C) and (D). Populations are YRI (green), CEU (orange), and CHB+JPT (purple). Shown are LOESS curves obtained for a span of 0.1 and a bin size of 1.2×10^{-5} cM. Above each figure is a histogram of the number of kilobases in each bin (plotted on a log scale). See (*20*) for alternative versions.

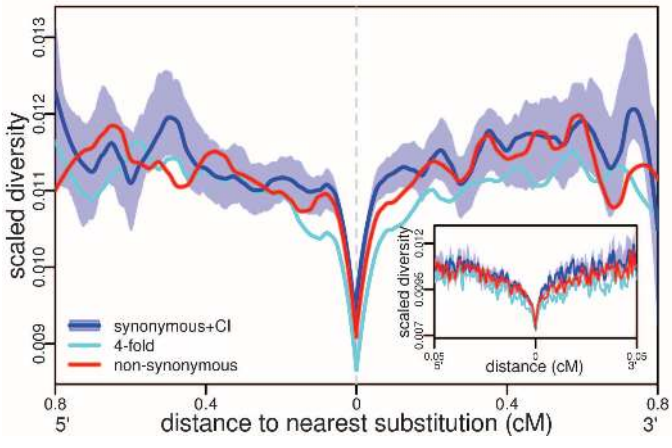

Fig. 2. CEU diversity levels divided by human–rhesus macaque divergence around human-specific substitutions, across autosomes. In the main plot, LOESS curves have a span of 0.2 and a bin size of 1.2×10^{-5} cM; the inset has a span of 0.05 to show added detail near the substitutions. The light blue shaded area represents the central 95th percentile of diversity estimates obtained from 100 bootstrap simulations. For alternative versions of this figure, including the same plot for YRI and CHB+JPT, as well as the X chromosome, see fig. S5.

If the trough in scaled diversity results from classic sweeps at linked sites, it should be deepest around those changes most likely to have functional consequences (i.e., within exons, around amino acid substitutions). We tested this prediction by considering the average scaled diversity around human-specific amino acid fixations and, as a control for other evolutionary forces, around synonymous substitutions. Our rationale was as follows: Human and chimpanzee species split approximately 5 million years ago [e.g., (*23*)], such that, assuming a constant rate of substitution, about 5% of human-specific substitutions could have left a detectable sweep in their wake (i.e., have occurred in the past 250,000 years). Thus, if a substantial fraction of amino acid changes are the result of classic sweeps, average diversity should be decreased around amino acid substitutions as compared to synonymous substitutions. In the fly *Drosophila simulans*, diversity levels are indeed significantly lower and suggest that ~13% of amino acid substitutions involved classic sweeps (*24*). In contrast, human diversity levels around amino acid substitutions are not lower than around synonymous substitutions (Fig. 2; $P = 0.90$ for a window of size 0.02 cM around the focal substitution). This conclusion is robust to alternative approaches for inferring substitutions or estimating divergence and to the choice of genetic map (fig. S5). The similar troughs indicate either that amino acid and synonymous mutations (including fourfold degenerate mutations; Fig. 2) experienced recurrent classic selective sweeps of similar intensities and rates or, more plausibly, that few amino acid substitutions resulted from classic sweeps.

Simulations suggest that even if only 10% of human-specific amino acid substitutions were strongly favored or if 25% of amino acid fixations were favored with weak effects, there should be a significant decrease in the diversity levels relative to what would be expected if all fixations were neutral (Fig. 3A) (*20*). These simulations mimic the data structure but do not fully capture the clustering of substitutions in the genome (fig. S6). Because amino acid substitutions are more clustered with one another than with synonymous substitutions (fig. S6A), this omission is conservative, leading to an underestimate of the power to detect the effects of classic sweeps (fig. S7) (*20*). Thus, our finding strongly constrains the maximal fraction of protein changes that could have resulted from classic sweeps in the past 250,000 years.

The troughs in diversity around both synonymous and amino acid fixations could instead be due to strong purifying selection at linked sites. Indeed, we found that under a model of back-

ground selection (*17*), the expected troughs are of similar depths to the observed ones, with lower diversity predicted around fourfold degenerate substitutions than around amino acid substitutions, as observed (Fig. 3B) (*20*). Interestingly, even though the model assumes extremely weak purifying selection in CNCs, it predicts a trough around them as well (fig. S8), indicating that the observed decrease in diversity around CNCs may primarily reflect selection on linked exons.

The prevalence of classic sweeps can also be evaluated by considering the genetic differentiation among the three population samples, whose ancestors occupied a range of environments. The two Eurasian populations [a population of European ancestry (CEU) and the combined Chinese and Japanese (CHB+JPT)] are thought to have split from the Yoruba (YRI) more than 100,000 years ago, and CEU and CHB+JPT are thought to have split about 23,000 years ago [e.g., (*25*)]. Given this time frame, local adaptation involving classic sweeps would have led to fixed differences or extreme differences in allele frequencies between YRI and CEU/CHB+JPT (and possibly between CEU and CHB+JPT) at targets of selection [see (*16*)]. Consistent with this expectation, there is an enrichment of highly differentiated single-nucleotide polymorphisms (SNPs) between population pairs in genic regions relative to nongenic regions (Fig. 4A) (*15*, *16*). However, the enrichments can also be explained by a 10 to 15% decrease in the effective population size near exons due to background selection (i.e., a trough similar to that in Fig. 1A) (*16*). In turn, CNCs are not significantly enriched for highly differentiated SNPs relative to nonconserved noncoding regions (Fig. 4B and fig. S9B).

Although the enrichment of genic SNPs could in principle result from purifying selection alone, there are well-documented examples of adaptations among the most highly differentiated SNPs, notably in genes involved in pigmentation or infectious disease susceptibility (*19*)—in other words, there are at least a handful of loci that conform to the sweep model. To ask whether these cases represent the tip of the iceberg of sweeps yet to be discovered, we tested for an enrichment of highly differentiated alleles that cause amino acid changes or that lie in putative regulatory regions, at which the highest fraction of changes would be expected, a priori, to have phenotypic consequences and hence to be possible targets of sweeps. Because CNCs may be unusual regulatory elements, we also considered SNPs in untranslated regions (UTRs) or 1 kb upstream of the transcription start site (TSS), annotations in which more than 10% of substitutions were estimated to be beneficial (*22*) and which are most strongly enriched for expression quantitative trait loci in cell lines (*26*). These annotations all fall within genic regions, so a test of enrichment against the genomic background is confounded by background selection or other modes of selection that increase population differentiation at genic sites. Nonetheless, in comparisons among the three human populations, enrichments of highly differentiated alleles at nonsynonymous sites, at 5′ and 3′ UTRs, and within 1 kb upstream of the TSS are either not significant or only marginally significant when tested against the genomic background (Fig. 4, C to F, and fig. S10). This finding reflects the small numbers of cases of highly differentiated alleles (fig. S11) and underscores how few local adaptations resulted from the extreme changes in allele frequencies among populations expected from classic sweeps. In particular, there are only four fixed amino acid differences between YRI and CEU, suggesting a rate of classic sweeps far below 10% since the two populations split [see (*20*)].

Moreover, the cases of extreme differentiation could also arise under an alternative model to the classic sweep, in which the beneficial allele was not a new mutation but was already segregating in the population. Although tests based on the frequency spectrum or the decay of linkage disequilibrium have low power to detect this mode of selection [e.g., (*6*, *27*)], measures of differentiation should have substantial power so long as there was little or no gene flow between the populations and the allele was at low frequency when first favored (*28*) (as is likely to be the case for both neutral and previously deleterious alleles). Intriguingly, the alleles with the largest differences in frequency between populations, which should be most enriched for targets of selection (*6*), often segregate in both populations (fig. S12) and tend to lie on a shorter haplotype

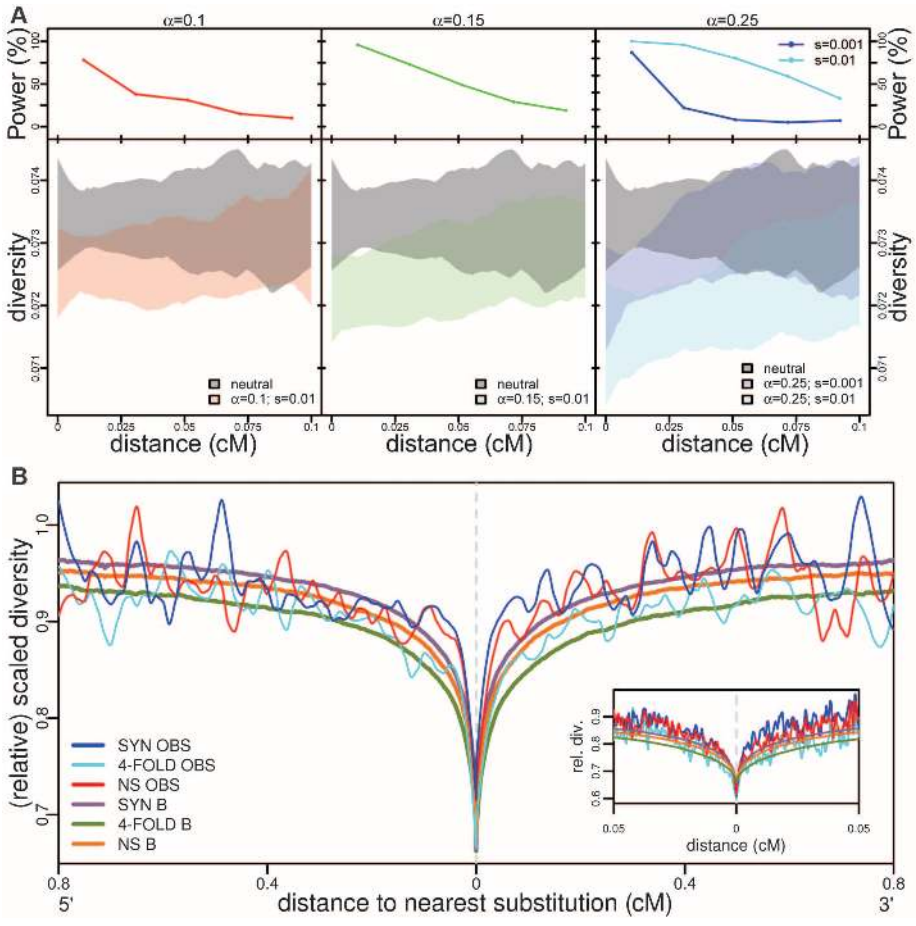

Fig. 3. (**A**) The power to detect a decrease in diversity levels around amino acid substitutions due to classic sweeps. The upper panels show the power at a given genetic distance from the substitution, for the three sets of selection parameters [see (*20*)]; the lower panels show the diversity patterns expected around amino acid substitutions for four sets of selection parameters, as well as for a model of purely neutral fixations, after LOESS smoothing (with a span of 0.2). For each set of parameters, the shaded area represents the central 95th percentile obtained from 100 bootstrap simulations. The depth of the trough reflects the fraction of substitutions that were beneficial; its width reflects the typical strength of selection (*24*). (**B**) Relative diversity levels around nonsynonymous, synonymous, and fourfold degenerate synonymous substitutions predicted under a model of background selection [see (*20*)]. The symbol B denotes the predicted diversity level relative to what is expected with no effects of background selection (i.e., under strict neutrality), taking into account variation in mutation rates (*11*). OBS refers to the observed value of average scaled diversity (i.e., diversity divided by human–rhesus macaque divergence). For the expected diversity around exons and CNCs, as well as predictions for the X chromosome, see fig. S8. The inset has a span of 0.05 to show added detail near the substitutions.

than expected from a classic sweep (*16*), consistent with selection on standing variation rather than ongoing classic sweeps.

In summary, patterns of diversity around genic substitutions and of highly differentiated alleles are inconsistent with the expectation for frequent classic sweeps, but could result, at least in part, from background selection. Thus, although some substitutions in proteins and regulatory positions undoubtedly involved classic sweeps, they were too infrequent within the past 250,000 years to have had discernible effects on genomic diversity.

This conclusion does not imply that humans have experienced few phenotypic adaptations, or that adaptations have not shaped genomic patterns of diversity. Comparisons of diversity and divergence levels at putatively functional versus neutral sites, for example, suggest that 10 to 15% [and possibly as many as 40% (*29*)] of amino acid differences between humans and chimpanzees were adaptive [e.g., (*30*)], as were 5% of substitutions in conserved noncoding regions (*22*, *29*) and ~20% in UTRs (*22*). Given the paucity of classic sweeps revealed by our findings, an excess of functional divergence would point to the importance of other modes of adaptation. One way to categorize modes of adaptation is in terms of their effect on the allele frequencies at sites that affect the beneficial phenotype. In this view, classic sweeps bring new alleles to fixation; selection on standing variation or on multiple beneficial alleles brings rare or intermediate frequency alleles to fixation; and other forms of adaptation, such as selection on polygenic traits, increase or decrease allele frequencies to a lesser extent. Such changes in allele frequencies can decrease variation at closely linked sites—to a lesser extent than in a full sweep—and might therefore contribute to a reduction in diversity near functional elements (*31*) as well as to excess divergence. Alternatives to classic sweeps are likely for parameters applicable to human populations (*7*, *32*); in particular, many phenotypes of interest are quantitative and plausibly result from selection at many loci of small effect (*8*).

An important implication is that in the search for targets of human adaptation, a change in focus is warranted. To date, selection scans have relied almost entirely on the sweep model, either explicitly (by considering strict neutrality as the null hypothesis and a classic sweep as the alternative) or implicitly (by ranking regions by a statistic thought to be sensitive to classic sweeps and focusing on the tails of the empirical distribution). It appears that few adaptations in humans took the form that these approaches are designed to detect, such that low-hanging fruits accessible by existing approaches may be largely depleted. Conversely, the more common modes of adaptation likely remain undetected. Thus, to dissect the genetic basis of human adaptations and assess what fraction of the genome was affected by positive selection, we need new tests to detect other modes of selection, such as comparisons between closely related populations that have adapted to drastically different environments [e.g., (*33*)] or methods that consider loci that contribute to the same phenotype jointly [e.g., (*34*)]. Moreover, if alleles that contribute to recent adaptations are often polymorphic within a population, genome-wide association studies should be highly informative.

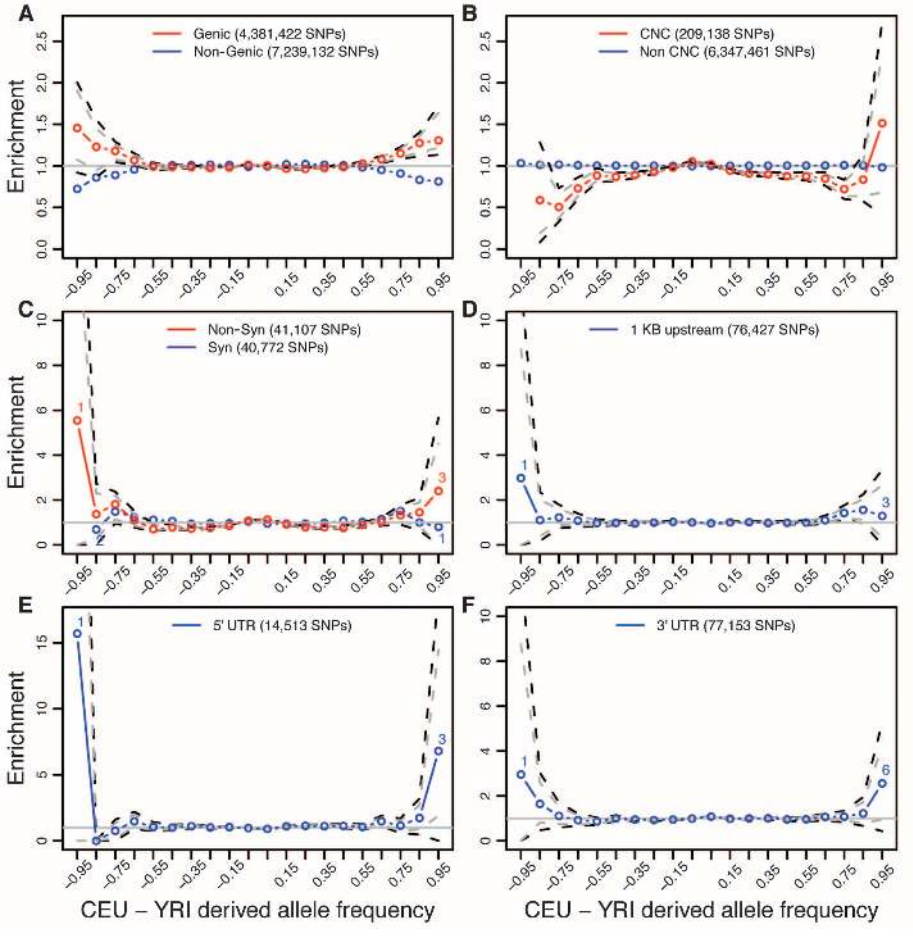

Fig. 4. (**A**) Enrichment of highly differentiated SNPs in genic relative to nongenic sites. Shown is the CEU-YRI comparison (other population comparisons are in fig. S9A). The total number of SNPs considered in each pairwise comparison is provided within each panel. Central 90% and 98% confidence intervals are shown with gray and black dashed lines, respectively; they were obtained by bootstrapping 200-kb regions 1000 times (*16*). (**B**) Enrichment of highly differentiated SNPs in conserved noncoding positions relative to nonconserved, noncoding positions (*20*) for the CEU-YRI comparison. Other population comparisons are in fig. S9B. (**C** to **F**) Enrichment of specific genic annotations relative to the genomic background for the CEU-YRI comparison, with central 90% and 98% confidence intervals shown as gray and black dashed lines, respectively. Note that an enrichment of 0 corresponds to no SNPs with that level of differentiation, and the confidence interval is not estimated in this case. Other population comparisons are shown in fig. S10. For the numbers of each bin, see fig. S11. Enrichments calculated on the folded frequency spectrum are shown in fig. S13B. For a comparison of synonymous and nonsynonymous SNPs in an alternative resequencing data set, see fig. S14.

References and Notes

1. P. C. Sabeti *et al.*, *Science* **312**, 1614 (2006).
2. J. M. Akey, *Genome Res.* **19**, 711 (2009).
3. J. Maynard Smith, J. Haigh, *Genet. Res.* **23**, 23 (1974).
4. M. Przeworski, *Genetics* **160**, 1179 (2002).
5. S. H. Williamson *et al.*, *PLoS Genet.* **3**, e90 (2007).
6. K. M. Teshima, G. Coop, M. Przeworski, *Genome Res.* **16**, 702 (2006).
7. J. Hermisson, P. S. Pennings, *Genetics* **169**, 2335 (2005).
8. J. K. Pritchard, J. K. Pickrell, G. Coop, *Curr. Biol.* **20**, R208 (2010).
9. I. Hellmann *et al.*, *Genome Res.* **18**, 1020 (2008).
10. J. J. Cai, J. M. Macpherson, G. Sella, D. A. Petrov, *PLoS Genet.* **5**, e1000336 (2009).
11. G. McVicker, D. Gordon, C. Davis, P. Green, *PLoS Genet.* **5**, e1000471 (2009).
12. A. Keinan, D. Reich, *PLoS Genet.* **6**, e1000886 (2010).
13. E. Santiago, A. Caballero, *Genetics* **169**, 475 (2005).
14. P. C. Sabeti *et al.*, International HapMap Consortium, *Nature* **449**, 913 (2007).
15. L. B. Barreiro, G. Laval, H. Quach, E. Patin, L. Quintana-Murci, *Nat. Genet.* **40**, 340 (2008).
16. G. Coop *et al.*, *PLoS Genet.* **5**, e1000500 (2009).
17. B. Charlesworth, M. T. Morgan, D. Charlesworth, *Genetics* **134**, 1289 (1993).
18. B. Charlesworth, M. Nordborg, D. Charlesworth, *Genet. Res.* **70**, 155 (1997).
19. R. M. Durbin *et al.*, 1000 Genomes Project Consortium, *Nature* **467**, 1061 (2010).

20. See supporting material on *Science* Online.
21. M. F. Hammer *et al.*, *Nat. Genet.* **42**, 830 (2010).
22. D. G. Torgerson *et al.*, *PLoS Genet.* **5**, e1000592 (2009).
23. N. Patterson, D. J. Richter, S. Gnerre, E. S. Lander, D. Reich, *Nature* **441**, 1103 (2006).
24. S. Sattath, E. Elyashiv, O. Kolodny, Y. Rinott, G. Sella, *PLoS Genet.* pgen.1001302 (2010).
25. R. N. Gutenkunst, R. D. Hernandez, S. H. Williamson, C. D. Bustamante, *PLoS Genet.* **5**, e1000695 (2009).
26. J. B. Veyrieras *et al.*, *PLoS Genet.* **4**, e1000214 (2008).
27. M. Przeworski, G. Coop, J. D. Wall, *Evolution* **59**, 2312 (2005).
28. H. Innan, Y. Kim, *Genetics* **179**, 1713 (2008).
29. A. Eyre-Walker, P. D. Keightley, *Mol. Biol. Evol.* **26**, 2097 (2009).
30. A. R. Boyko *et al.*, *PLoS Genet.* **4**, e1000083 (2008).
31. E. Santiago, A. Caballero, *Genetics* **139**, 1013 (1995).
32. P. L. Ralph, G. Coop, *Genetics* **186**, 647 (2010).
33. G. H. Perry *et al.*, *Nat. Genet.* **39**, 1256 (2007).
34. H. A. Orr, *Genetics* **149**, 2099 (1998).
35. We thank G. Coop, T. Long, G. McVicker, J. Pickrell, J. Pritchard, and K. Thornton for helpful discussions, and G. Coop, A. Di Rienzo, and J. Pritchard for comments. Supported by an NSF minority postdoctoral fellowship (R.D.H.), National Research Service Award postdoctoral fellowship GM087069 (J.L.K.), Wellcome Trust grant WT086084MA (G.M.), Israeli Science Foundation grant 1492/10 and NIH grant GM083228 (G.S.), and NIH grants GM20373 and GM72861 (M.P.). M.P. is a Howard Hughes Medical Institute Early Career Scientist.

Supporting Online Material

www.sciencemag.org/cgi/content/full/331/6019/920/DC1
Materials and Methods
Figs. S1 to S16
References

12 October 2010; accepted 6 January 2011
10.1126/science.1198878

Early Tagging of Cortical Networks Is Required for the Formation of Enduring Associative Memory

Edith Lesburguères, Oliviero L. Gobbo, Stéphanie Alaux-Cantin, Anne Hambucken, Pierre Trifilieff, Bruno Bontempi*

Although formation and stabilization of long-lasting associative memories are thought to require time-dependent coordinated hippocampal-cortical interactions, the underlying mechanisms remain unclear. Here, we present evidence that neurons in the rat cortex must undergo a "tagging process" upon encoding to ensure the progressive hippocampal-driven rewiring of cortical networks that support remote memory storage. This process was AMPA- and *N*-methyl-D-aspartate receptor–dependent, information-specific, and capable of modulating remote memory persistence by affecting the temporal dynamics of hippocampal-cortical interactions. Post-learning reinforcement of the tagging process via time-limited epigenetic modifications resulted in improved remote memory retrieval. Thus, early tagging of cortical networks is a crucial neurobiological process for remote memory formation whose functional properties fit the requirements imposed by the extended time scale of systems-level memory consolidation.

Memories for facts and events are not acquired in their definitive form but undergo a gradual process of stabilization over time (*1*–*3*). According to the so-called standard theory of systems-level memory consolidation, the hippocampus (HPC) is believed to integrate, in the form of an anatomical index, information transmitted from distributed cortical networks that support the various features of a whole experience (*4*). Upon encoding, the HPC rapidly fuses these different features into a coherent memory trace. Consolidation of this new memory trace at the cortical level would then occur slowly via repeated and coordinated reactivation of hippocampal-cortical networks in order to progressively increase the strength and stability of cortical-cortical connections that represent the original experience. Over days to weeks as memories mature, the role of the HPC would gradually diminish, presumably leaving cortical areas to become capable of sustaining permanent memories and mediating their retrieval independently (*4*, *5*). Using brain imaging, we have provided evidence supporting the time-limited role of the HPC as a consolidation organizing device of remote memory in the cortex (*5*, *6*). Yet the nature and dynamics of plasticity phenomena as well as the neuronal constraints within hippocampal-cortical networks responsible for the formation of remote memories have remained elusive.

To pinpoint the post-learning mechanisms underlying the hippocampal-cortical dialogue during the course of systems-level memory consolidation, we used the social transmission of food preference (STFP) paradigm, which involves an ethologically based form of associative olfactory memory (*7*). In this task, rats learn, within only one single interaction session of 30 min, about the safety of potential food sources by sampling the odor of those sources on the breath of littermates (*8*). After establishing the necessary role played by the HPC in acquisition of associative olfactory memory (*9*) (fig. S1), we trained independent groups of rats and tested them for memory retrieval either 1 day (recent memory) or 30 days (remote memory) later. Interaction of experimental observer rats with a demonstrator rat fed with cumin reversed the innate preference typically expressed by control observer rats (food preference), which interacted with a demonstrator rat fed with plain food (fig. S2A). The acquired memory for cumin was robust and long-lasting, which makes the STFP task particularly suitable to studying the processes underlying remote memory formation. Cellular imaging of the activity-dependent gene *c-fos* (*6*) coupled to region-specific pharmacological inactivation of HPC by using tetrodotoxin or the AMPA receptor antagonist 6-cyano-7-nitroquinoxaline-2,3-dione (CNQX) revealed a transitory role of this region in remote memory storage of associative olfactory information (figs. S2, B to D, and S3). At the cortical level, we focused our analyses on the orbitofrontal cortex (OFC) because of its privileged role in processing the relevance of associative olfactory information (fig. S2E) (*10*). The observed hippocampal disengagement was associated with a concomitant increase in Fos immunoreactivity in the OFC (fig. S2B). Accordingly, inactivation of the OFC selectively impaired remote memory retrieval (figs. S2, C and D, and S3). Although a broad cortical network is likely to be involved in the processing of remote associative olfactory memory, our results identify the OFC as a critical node within this network. Concurring with this, we found neuronal networks of the OFC to undergo time-dependent morphological changes at pre- and postsynaptic sites (fig. S4).

To determine whether such a progressive synaptic remodeling in the OFC during remote memory storage is driven by the HPC, we chronically inactivated the dorsal HPC during two critical post-learning periods: an early (from day 0 to day 12) and a late (from day 15 to day 27) time window (Fig. 1A). This reversible pharmacological approach enabled us to target selectively post-learning consolidation mechanisms without interfering with retrieval processes (fig. S3). Remote memory retrieval examined at day 30 was impaired when hippocampal activity was silenced during the early, but not the late, post-learning period (Fig. 1B and fig. S5). This early hippocampal dysfunction also completely abolished the late development of dendritic spine growth on OFC neurons (Fig. 1B). Delaying intrahippocampal infusion of CNQX by 1 day so as to prevent any confounding interference with cellular consolidation mechanisms (*1*, *2*, *5*) that were triggered immediately upon encoding yielded similar results (fig. S6). Therefore, these findings

Institut des Maladies Neurodégénératives, CNRS UMR 5293, Universités Bordeaux 1 et 2, Avenue des Facultés, 33405 Talence, France.

*To whom correspondence should be addressed. E-mail: bruno.bontempi@u-bordeaux2.fr